

# Modeling pion and proton total cross-sections at LHC

A. Grau<sup>a</sup>, G. Pancheri<sup>b</sup>, O. Shekhovstova<sup>b</sup>, Y. N. Srivastava<sup>c</sup>

<sup>a</sup>*Departamento de Física Teórica y del Cosmos, Universidad de Granada, Spain*

<sup>b</sup>*INFN Frascati National Laboratories, P.O. Box 13, Frascati I00044, Italy*

<sup>c</sup>*Physics Department and INFN, University of Perugia, Perugia I06123, Italy*

---

## Abstract

To settle the question whether the growth with energy is universal for different hadronic total cross-sections, we present results from theoretical models for  $\pi p$ , and  $(pp, p\bar{p})$  total cross-sections. We show that present and planned experiments at LHC can differentiate between different models, all of which are consistent with presently available (lower energy) data. This study is also relevant for the analysis of those very high energy cosmic ray data which require reliable  $\pi p$  total cross-sections as seeds. A preliminary study of the total  $\pi\pi$  cross-sections is also made.

*Keywords:* Hadronic total cross-section, QCD minijets, Soft Gluon Resummation, Froissart bound

---

## 1. Introduction

In the present work we describe theoretical predictions for total pion-nucleon cross-sections at LHC using our eikonal mini-jet model with soft gluon  $k_t$ -resummation [1, 2]. We shall show that at very high energy there is considerable difference between current fits and our QCD based model. We shall also present a preliminary estimate for the pion-pion cross-sections.

Recently a number of papers have appeared which point both to the interest [3] and the feasibility of measuring pion cross-sections at LHC [4, 5]. The proposal for LHC as a “pion collider” [3] and measurements of  $\pi N$  and even  $\pi\pi$  scattering in the TeV range is based on the mechanism of pion

---

*Email addresses:* [igrau@ugr.es](mailto:igrau@ugr.es) (A. Grau), [pancheri@lnf.infn.it](mailto:pancheri@lnf.infn.it) (G. Pancheri), [shekhovtsova@lnf.infn.it](mailto:shekhovtsova@lnf.infn.it) (O. Shekhovstova), [yogendra.srivastava@pg.infn.it](mailto:yogendra.srivastava@pg.infn.it) (Y. N. Srivastava)

exchange (single and double) and detection of neutral particles in the forward direction. Dedicated experiments such as the Zero Degree Calorimeter (ZDC) experiment [6], will place their detectors in the very forward region, a few micro radians from the beam and measure photons,  $\pi^0$ 's and neutrons. Detecting neutrons, total pion- proton and pion-pion cross-sections could be measured through the pion exchange mechanisms as shown in Fig. 1.

Extraction of the  $\pi p$  total cross-section was suggested long time ago [7], rediscussed later in [8] and measured in  $\gamma p \rightarrow \pi^+ \pi^- p$  at HERA [9]. At CERN ISR, the measurement of the inclusive zero-angle neutron spectra gave strong experimental support [10] to the presence of an important charge exchange mechanism in the forward direction. This analysis was based on measurements of the inclusive differential cross-section for  $pp \rightarrow nX$  at zero degree production angle and application of the triple Regge exchange mechanism to determine the exchanged trajectory  $\alpha(t)$ . In the kinematic limit of small  $M^2/s$ , but large  $M^2$ ,  $s$  one can write

$$\pi E \frac{d^3\sigma}{d^3p} \approx \frac{d^2\sigma}{dt d(M_X^2/s)} = |G(t)|^2 \left(\frac{M^2}{s}\right)^{1-2\alpha(t)} \sigma_{tot}(M^2, t) \quad (1)$$

where  $G(t)$  is the residue for the exchange of a reggeon between the proton and a neutron. One can interpret  $\sigma_{tot}(M^2, t)$  as the total reggeon scattering cross-section at a CM energy  $M$  and reggeon mass  $|t|$ . Fits to the data indicated a value for the trajectory intercept at  $t = 0$  of  $\alpha(0) = 0.11 \pm 0.15$ , consistent with the pion trajectory. Studies of the neutron spectra at HERA [11, 12] revived interest to the idea of using zero degree neutron detection to study pion exchange processes. Recently, forward neutron detection was examined in [13], and the extraction of the cross-section was discussed and a disagreement by a factor about 2 with the ISR data claimed. The data analyzed were forward neutron spectra from HERA [14, 15] and NA49 [16].

To have data for pion cross-sections in the TeV range would be very interesting as it could help to effectively discriminate among models by studying more types of hadrons in the initial state in a similar energy range. Predictions for the total  $pp$  cross-section at LHC energies vary from 90  $mb$  to 140  $mb$  and more, with some models claiming even lower values and other somewhat higher ones. LHC is expected to measure the total proton-proton cross-section with a precision of 5% within the next 3 years, down to a precision of 1 % when machine conditions at LHC will allow for it [17]. Such measurements should allow to discriminate among models. An additional strategy relies on comparing different initial states, such as photons or heavy

ions, and their total cross-section value at very high energy. Valuable as they are however, data from photons or heavy ion collisions require additional modelling, and this may cloud the issue. Pions, on the other hand, should make a cleaner comparison to proton results. Also, reliable total pion-nucleon cross-sections are needed for many cosmic ray analyses as well.

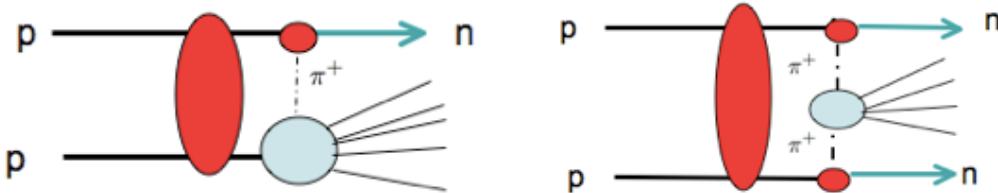


Figure 1: The pion exchange processes which would allow the measurement of  $\pi^+p$  and  $\pi^+\pi^+$  total cross-sections at LHC

## 2. The eikonal mini-jet model with soft gluon $k_t$ -resummation

We shall discuss total  $\pi N$  cross-sections from a few GeV to about 100 TeV CM energy range, and compare some current fits to results from our eikonal mini-jet model implemented with soft gluon resummation in the infrared region [1, 2]. This model has two major advantages or differences with respect to other mini-jet models. First, it explicitly probes the large distance region through soft gluon resummation in the infrared. We call it the Bloch-Nordsieck (BN) model because it relies on the role played by soft quanta resummation. We were inspired to build our model by the classic work of Bloch and Nordsieck [18] in electrodynamics, where they first pointed out that only the emission of an infinite number of soft photons can lead to a finite result. In our model [2], resummation and implementation of soft gluon  $k_t$ -resummation down into the gluon infrared momentum region constitute the mechanisms through which the fast initial rise of all total cross-sections is transformed into a smooth logarithmic behaviour, which satisfies the Froissart bound. The second point in favour of our approach is the calculation of the mini-jet cross-sections using actual Parton Density Functions (PDFs) from available libraries, and inclusive of DGLAP evolution. Thus, we can make predictions for different processes simply by introducing the proper PDFs in the formalism. Since the early observation of the rise of the total cross-section, parton-parton collisions were considered to be at the origin of the rise

[19]. QCD provides an obvious mechanism for this rise through the increasing number of low-energy perturbative gluon-gluon collisions, producing the so called *mini-jets* [20]. How to link these cross-sections to the total cross-section, without violating unitarity, was first done in the mid 80s through the eikonal mini-jet model [21, 22]. Mini-jet models are used in MonteCarlo simulation programs for very high energy collisions [23], although there are some unsolved problems concerning the elastic and diffractive components of the scattering, as recently summarized in [24]. We shall not address these issues here and apply the mini-jet model only to the total cross-section. For this purpose, we begin with the inelastic cross-section and then, using the fact that the real part of the scattering amplitude is expected to be small in the region of interest, we construct the model for the total cross-section, with the eikonal expression

$$\sigma_{total} \approx 2 \int d^2\vec{b} [1 - e^{-\bar{n}(b,s)/2}] \quad (2)$$

The simplest possible form for  $\bar{n}(b, s)$  being to write  $\bar{n}(b, s) = A(b)\sigma(s)$ , one can see how the QCD mini-jet cross-sections would contribute to inelastic collisions at high energy as the driving term in the rise of  $\sigma_{tot}$ . For scattering of particles A and B, an approximate expression from the low,  $\sqrt{s} \approx 5 \text{ GeV}$ , to the highest energies is

$$\bar{n}^{AB}(b, s) = \bar{n}_{soft}^{AB}(b, s) + \bar{n}_{QCD}^{AB}(b, s) = \bar{n}_{soft}^{AB}(b, s) + A_{BN}^{AB}(b, s)\sigma_{jet}^{AB}(s, p_{tmin}) \quad (3)$$

where  $p_{tmin}$  ( $\sim 1-2 \text{ GeV}$ ) is the cut-off in the mini-jet cross-section  $\sigma_{jet}^{AB}(s, p_{tmin})$ .

As mentioned, and recently described in [2], we obtain  $\sigma_{jet}^{AB}(s, p_{tmin})$ , and hence the rise of the total cross-section, through parton-parton scattering convoluted with Parton Density Functions (PDFs) from PDFLIB, properly evolved with the scale of outgoing parton transverse momentum. These are the mini-jet cross-sections in our model, and different initial state particles can be studied simply by changing the PDFs.

To obtain a rate of increase with energy such as to describe both the early rise as well as the subsequent logarithmic behaviour, we introduce soft  $k_t$ -resummation as the mechanism which generates an energy dependent acollinearity (and thus reduces the mini-jet cross-section) and write

$$A_{BN}^{AB}(b, s) = \frac{e^{-h(b, q_{max})}}{\int d^2\vec{b} e^{-h(b, q_{max})}} = \frac{\exp\left\{-\frac{16}{3\pi} \int_0^{q_{max}} \frac{dk_t}{k_t} \alpha_{eff}(k_t) \ln\left(\frac{2q_{max}}{k_t}\right) [1 - J_0(bk_t)]\right\}}{\int d^2\vec{b} e^{-h(b, q_{max})}} \quad (4)$$

where the function  $h(b, q_{max})$  is obtained from soft gluon resummation techniques [1], as indicated by the subscript  $BN$  which recalls the physics behind this function. The function  $h(b, q_{max})$  has a logarithmic energy dependence through the scale  $q_{max}$ , which is proportional to  $p_{tmin}$ . The excessive rise from the minijets is however reduced only by extending resummation to near zero soft gluon momenta, and this is accomplished through an *ad hoc* coupling, singular, but integrable, in place of the asymptotic freedom expression for  $\alpha_s$  in the soft gluon integral. With an effective coupling  $\alpha_{eff}(k_t) \sim k_t^{-2p}$  for the single soft gluon transverse momentum in the region  $0 \leq k_t \leq \Lambda_{QCD}$  and  $1/2 < p < 1$ , we have shown in [2] how this expression for  $A_{BN}^{AB}(b, s)$  introduces a strong cut-off in  $b$ -space and changes the violent rise of mini-jets into a smooth behavior in the total cross-section. Namely, we found that  $\sigma_{tot} \sim (\ln s)^{1/p}$ , a behaviour consistent with the limitations imposed by the Froissart bound.

To summarize, our model for  $\bar{n}_{QCD}^{AB}(b, s)$  is controlled by three different momentum regions:

1.  $p_t \geq p_{tmin}$ , for parton parton collisions, where a perturbative QCD description is applied, with  $p_{tmin} \sim (1 - 2) \text{ GeV}$  kept fixed and independent of energy;
2.  $\Lambda_{QCD} \leq k_t \leq q_{max}$  for single soft gluons emitted from initial state quarks before the hard parton-parton collision, with [1]  $q_{max} \sim p_{tmin} \ln \sqrt{s}/p_{tmin}$ ;
3.  $k_t \leq \Lambda_{QCD}$  for ultrasoft gluons in a region which is dominated by an effective singular, but integrable, coupling of the gluons with the emitting quarks.

The parameters which control the high energy rise of  $\bar{n}_{QCD}^{AB}(b, s)$  are then

- choice of PDFs (when different sets are available)
- $p_{tmin}$
- the singularity controlling parameter  $p$ .

Finally, in this paper we use

$$\bar{n}_{soft}^{AB}(b, s) = A_{FF}^{AB}(b) \sigma_{soft}^{AB}(s) \quad (5)$$

with the  $b$ -distribution given by the convolution of the form factors of the colliding particles. For protons and pions, this gives

$$A_{FF}^{pp}(b) = \frac{\nu^2(\nu b)^3}{96\pi} \mathcal{K}_3(b\sqrt{\nu^2}), \quad A_{FF}^{\pi\pi}(b) = \frac{q_0^3 b}{4\pi} \mathcal{K}_1(bq_0)$$

Table 1: Results of the fit to  $pp$ ,  $p\bar{p}$  data

Process	Fit
$pp$	$A_0 = (48.20 \pm 0.19)$ mb $A_1 = 101.66 \pm 16.35$ $\alpha_1 = 0.99 \pm 0.13$ $A_2 = 27.89 \pm 4.78$ $\alpha_2 = 0.59 \pm 0.04$ $\chi^2 = 154.1/(102 + 5 - 1)$
$p\bar{p}$	$A_0 = (47.86 \pm 2.47)$ mb $A_1 = 132.07 \pm 32.89$ $\alpha_1 = 0.69 \pm 0.14$ $A_2 = 0.82 \pm 0.31$ $\alpha_2 = 0.52 \pm 0.07$ $\chi^2 = 24.65/(31 + 5 - 1)$

$$A_{FF}^{\pi p}(b) = \frac{1}{4\pi} \frac{\nu^2 q_0^2}{q_0^2 - \nu^2} \left[ \nu b \mathcal{K}_1(\nu b) - \frac{2\nu^2}{q_0^2 - \nu^2} [\mathcal{K}_0(\nu b) - \mathcal{K}_0(q_0 b)] \right] \quad (6)$$

with  $\nu^2 = 0.71 \text{ GeV}^2$  for the proton and  $q_0 = 0.735 \text{ GeV}$  for the pion. At low energy, we parametrize the cross-section in the eikonal as

$$\sigma_{soft}^{AB}(s) = A_0 + \frac{A_1}{E_{lab}^{\alpha_1}} - \frac{A_2}{E_{lab}^{\alpha_2}} \quad (7)$$

and  $E_{lab} = \frac{s - m_A^2 - m_B^2}{2m_A}$  for particle B on fixed target A. In Eq. (7), the coefficients  $A_i$  and the exponents  $\alpha_i$  are in principle different for each different process. Following our analyses in [25, 26], we chose the set of high energy parameters given by GRV densities and set  $\{1,5,4\}$  [27],  $p_{tmin} = 1.15 \text{ GeV}$  and  $p = 0.75$ . We then applied Eqs. 6,7 to determine the low energy parameters for  $pp$  and  $p\bar{p}$  scattering and performed a best fit to the overall data set. The results of the fit for the low energy parameters are shown in Table 1.

Our curves are shown in Fig. 2 together with fits by Pelaez and Yndurain [PY] [28] for the combination  $(pp + p\bar{p})/2$ . These fits are part of a global fit to  $\pi\pi, \pi N, KN$  and  $pp, p\bar{p}$ . The PY fits follow Regge theory constraints in the low energy region and incorporate a high energy term which follows a more stringent limit [29] than the one imposed by the Froissart bound, i.e.

$$\sigma_{PY} = a_0 + a_1 s^{\beta_1} + a_2 s^{\beta_2} + B_{PY} \ln^2 \frac{s}{s_1 \ln^{7/2} s/s_2} \quad (8)$$

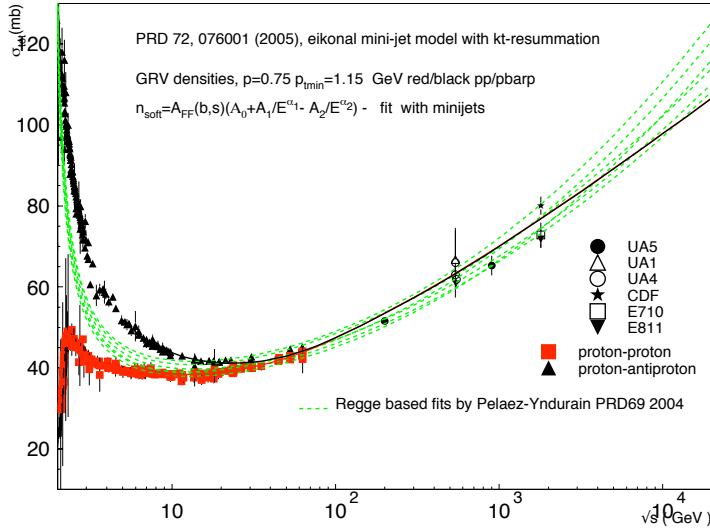


Figure 2: Results of our model for  $pp$  and  $\bar{p}p$  scattering compared with data and with Regge-based fits by Pelaez and Yndurain [28]. Fits for low energy parameters are in the variable  $E \equiv E_{lab}$ .

In our model, on the other hand, and as discussed before, we do not impose *a priori* the presence of any logarithmic term, rather we can see that at high energy the model naturally develops a logarithmic behaviour, not present in the low energy terms.

Having thus recalled the basic formulae which we shall use for extension of our model to pion processes, we describe in the next section what the model predicts for pion-proton cross-sections in the very high energy region, accessible through LHC as well as cosmic ray experiments, and compare our predictions with available parametrizations.

### 3. Phenomenology of $\pi p$ total cross-sections : comparing models and their predictions into the TeV range

In this section we apply our model, as described in the previous section, to  $\pi p$  scattering, comparing it with existing data, models and fits. Data from fixed target experiments [30] are available up to  $\sqrt{s} = 36.7 \text{ GeV}$  for  $\pi^- p$  and  $\sqrt{s} = 25.3 \text{ GeV}$  for  $\pi^+ p$ . A second set of data in the range  $9.4 \text{ GeV} \leq \sqrt{s} \leq 70 \text{ GeV}$  is the one obtainable from the charge exchange mechanism [3] described in the introduction. We examine four predictions for  $\pi^+ p$  total cross-section at LHC energies, namely:

- a Regge-Pomeron fit from Donnachie and Landshoff [31]

$$\sigma_{\pi^+p}(mb) = 13.63s^{0.0808} + 27.56s^{-0.4525} \quad (9)$$

noting that for  $\pi^-p$  the coefficient of the second (“Regge”) term is changed from 27.56 to 36.02;

- the fit from the COMPETE/PDG 2008 collaboration [30] given as

$$\sigma_{\pi^+p} = Z^{\pi p} + B \ln^2\left(\frac{s}{s_0}\right) + Y_1^{\pi p} \left(\frac{s_1}{s}\right)^{\eta_1} - Y_2^{\pi p} \left(\frac{s_1}{s}\right)^{\eta_2} \quad (10)$$

with  $Z^{\pi p} = 20.86 \text{ mb}$ ,  $B = 0.308 \text{ mb}$ ,  $Y_1^{\pi p} = 19.24 \text{ mb}$ ,  $Y_2^{\pi p} = 6.03 \text{ mb}$ ,  $\eta_1 = 0.458$ ,  $\eta_2 = 0.545$ ,  $s_1 = 1 \text{ GeV}^2$ ,  $\sqrt{s_0} = 5.38 \text{ GeV}$

- a fit by Block and Halzen [32] with a functional expression similar to the one from PDG but with an extra term linear in  $\ln s$ ,

$$\sigma^{ab} = c_0 + c_1 \ln(\nu/m_\pi) + c_2 \ln^2(\nu/m_\pi) + \beta(\nu/m_\pi)^{\eta_1} + \delta(\nu/m_\pi)^{\eta_2} \quad (11)$$

with numerical coefficients for  $\pi^+p$  given by  $c_0 = 20.11 \text{ mb}$ ,  $c_1 = -0.921 \text{ mb}$ ,  $c_2 = 0.1767 \text{ mb}$ ,  $\beta = 54.4 \text{ mb}$ ,  $\delta = -4.51 \text{ mb}$ ,  $\eta_1 = -0.5$ ,  $\eta_2 = -0.34$  and  $\nu$  the laboratory energy;

- the eikonal mini-jet model with initial state soft gluon  $k_t$ -resummation described in the previous section, with GRV density functions for both the pion [33] and the proton [27].

We shall now enter more into the details of our calculation. We proceed to study  $\pi^+p$  and  $\pi^-p$  by fitting the low energy part of the eikonal function,  $\bar{n}_{soft}^{AB}$ , with  $A_0^{\pi p}$  either fixed to  $2/3 A_0^{pp}$ , following the Additive Quark Parton Model (AQPM) rule, or free to vary, and the high energy part  $\bar{n}_{QCD}^{AB}$  computed with the same parameters used for  $pp$  or  $\bar{p}p$ , except that the PDFs are now those for pions. Thus, we used  $p_{tmin} = 1.15 \text{ GeV}$ ,  $p = 0.75$ , and GRV densities for pions and protons. Then, through a fit which includes the minijet contribution in the eikonal, we determine the low energy parameters entering  $\bar{n}_{soft}^{\pi^{\pm}p}$ . The low energy part of the cross-section is as before obtained through Eqs. 6 and 7. Notice that this procedure includes the rise due to mini-jets even when their contribution is too small to be actually detected.

The scope of this exercise is twofold: to see whether the AQPM rule works for the constant term of the eikonal function, and obtain predictions



Table 2: Results of the fit to  $\pi^+p$ ,  $\pi^-p$  data.

Process	Fit 1, fixed value of $A_0$ equal to $A_0 = \frac{2}{3}A_0(pp)$	Fit 2 free value of $A_0$
$\pi^+p$	$A_0 = 32$ mb $A_1 = 37.9 \pm 2.4$ $\alpha_1 = 0.46 \pm 0.02$ $A_2 = 24.6 \pm 0.96$ $\alpha_2 = 0.20 \pm 0.01$ $\chi^2 = 70/(50 + 4 - 1)$	$A_0 = (28.5 \pm 0.13)$ mb $A_1 = 80.8 \pm 1.1$ $\alpha_1 = 0.52 \pm 0.05$ $A_2 = 58.9 \pm 0.95$ $\alpha_2 = 0.40 \pm 0.004$ $\chi^2 = 69.5/(50 + 5 - 1)$
$\pi^-p$	$A_0 = 32$ mb $A_1 = 37.4 \pm 4.5$ $\alpha_1 = 0.41 \pm 0.03$ $A_2 = 20.8 \pm 4.8$ $\alpha_2 = 0.16 \pm 0.02$ $\chi^2 = 193/(95 + 4 - 1)$	$A_0 = (27.4 \pm 0.1)$ mb $A_1 = 84.4 \pm 0.7$ $\alpha_1 = 0.57 \pm 0.02$ $A_2 = 55.5 \pm 1.7$ $\alpha_2 = 0.50 \pm 0.02$ $\chi^2 = 197/(95 + 5 - 1)$

for the high energy behaviour based on the same parameter set as in  $pp$  or  $\bar{p}p$ . We do not actually know whether the high energy parameters should be the same for all processes or be energy independent, but keeping them fixed, as we do, can give information about their universality. The result for these two different ways to study  $\pi p$  scattering at high energy is then examined by the  $\chi^2$  for the two different cases,  $\pi^-p$  and  $\pi^+p$ . We show the results of the fit in Table 2.

We find that one obtains a good fit to the data in either of the two cases,  $A_0$  free or given by the AQPM rule of  $2/3$ . Before proceeding further, we notice a difference between our result for the low energy fit and other fits: our constant term  $A_0$  can fit the data with a value  $\approx 2/3$  of the constant term used in the eikonal for  $pp$  and  $\bar{p}p$ , while the other fits (PDG and BH), have a ratio of the constant terms  $< 2/3$ . This may be due to the fact that they assume the contribution of a  $\ln^2 s$  or  $\ln s$  term throughout the entire energy region, whereas in our model the logarithmic behaviour arises naturally through the minijets and the  $k_t$ -resummation effect mentioned in the previous section and described in [2]. Such terms, although present in the fitting procedure, start contributing only for  $\sqrt{s} \geq 10$  GeV.

In Fig. 3 we compare the fits labelled DL, BH and PDG with existing data for  $\pi^+p$  and with the results from our model. We show a comparison in the low energy region, where there are data, and the high energy predictions. The points labelled PRS are from [3] and have been extracted from actual

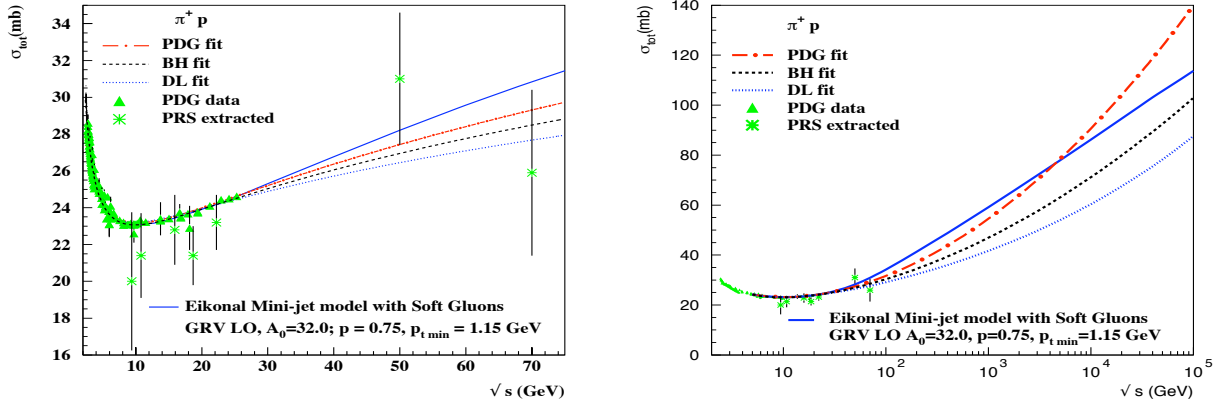


Figure 3: In the left panel we show the fit for  $\pi^+p$  channel in the low energy region when the parameter  $A_0$  is fixed to the value  $2/3 A_0^{pp}$ , and with values of the low energy parameters as in Table 2. At right, we show the full energy range of interest.

data, BH is the fit from [32], and DL from [31]. We show the case  $A_0$  fixed according to the AQPM model, but, as mentioned, there is no discernible difference in the results when  $A_0$  is free to vary.

We notice that there is a difference of almost a factor 2 among the asymptotic limit of different curves, indicating the interest of this exercise. This difference is of course due to the fact that data for  $\pi p$  extend only up to the beginning of the rise and fits cannot really adequately determine the asymptotic behaviour. The situation here is quite different from the  $pp$  case where data constrain the LHC value to within a 10-20% range, an uncertainty carried on from the Tevatron data. The extension of our investigation to energies in the very high cosmic ray region, namely up to  $\sqrt{s} \sim 100 \text{ TeV}$  shows that at this energy there is no difference, as expected, between  $\pi^+p$  and  $\pi^-p$  cross-sections, but an even larger difference among different fits and our model is observed. We reproduce these results in Table 3.

#### 4. $\pi\pi$ scattering

The possibility to measure elastic  $\pi^+\pi^+$  scattering at LHC has recently been discussed at some length [5]. A related exclusive cross-section measurement for the process  $pp \rightarrow nn\pi^+\pi^+$  is discussed in [4]. At a  $p\bar{p}$  collider

Table 3: Total  $\pi^\pm p$  cross-section at  $\sqrt{s} = 100 \text{ TeV}$

Model	Value in mb	Value in mb
	$\pi^- p$	$\pi^+ p$
PDG	139.9	139.9
BH	102.89	102.88
DL	87.59	87.59
EMM (fixed A0)	113.72	113.75
EMM (free A0)	113.28	113.40

(such as the Tevatron), one has in principle the possibility of obtaining the cross-section for the channel  $\pi^+\pi^-$  through the process  $p\bar{p} \rightarrow n\bar{n}\pi^+\pi^-$ . One may even entertain the possibility of measuring -at the LHC- the neutral  $\pi^+\pi^-$  channel via the measurement  $pp \rightarrow n\Delta^{++}\pi^+\pi^-$  and the  $\pi^+\pi^0$  channel via the reaction  $pp \rightarrow n\Delta^+\pi^+\pi^0$ .

A good overview of the available total cross-section data for like-sign and opposite sign  $\pi\pi$  at low energy is summarized in [28]. There are no data for the process  $\pi^+\pi^+$  but isospin invariance tells us that the cross-section is the same as the one for  $\pi^-\pi^-$ , for which there exist data which we shall then use for a fit. However, unlike the other scattering processes we considered until now, data for the  $\pi\pi$  channels [34, 35, 36, 37, 38, 39] do not extend into the region where minijets start playing a role and, in addition, these data are in some contradiction with each other and have large errors. This makes fits and the error analysis particularly difficult, and the extension to higher energies uncertain. We shall return to a detailed investigation of this point in subsequent work.

With the above *caveats*, we follow the strategy presented before and perform a fit to the data to determine the low energy parameters. Starting with  $\pi^+\pi^-$  and leaving  $A_0$  free, we obtain

$$A_0^{\pi^+\pi^-} = (22.0 \pm 9.8) \text{ mb}, \quad A_1 = 100.0 \pm 89.8, \quad \alpha_1 = 0.74 \pm 0.66, \quad (12)$$

$$A_2 = 27.8 \pm 49.1, \quad \alpha_2 = 0.27 \pm 0.33 \quad (13)$$

with  $\chi^2 = 6.93/(17 + 5 - 1)$ . The  $\pi^+\pi^-$  fit done leaving  $A_0$  free gives a central value  $A_0^{\pi\pi} = 4/9 A_0^{pp}$  as expected from the AQPm rule. However, the parameters for  $\pi\pi$  are determined with large errors. In this paper, we have presented results from our model using the best mean values for the fitted parameters. The encouraging results which we obtain justify *a fortiori* such

Table 4: Results of the fit to  $\pi^-\pi^-$  data.

Process	Fit 1, fixed value of $A_0$ equal to free fit value for $A_0(\pi^+\pi^-)$	Fit 2 free value of $A_0$
$\pi^-\pi^-$	$A_0 = 22.0$ mb $A_1 = 85.5 \pm 1.1$ $\alpha_1 = 0.08 \pm 0.08$ $A_2 = 99.7 \pm 0.9$ $\alpha_2 = 0.08 \pm 0.07$ $\chi^2 = 53.19/(14 + 4 - 1)$	$A_0 = (12.3 \pm 0.2)$ mb $A_1 = 80.2 \pm 2.1$ $\alpha_1 = 0.53 \pm 0.004$ $A_2 = 99.9 \pm 0.02$ $\alpha_2 = 0.57 \pm 0.001$ $\chi^2 = 49.19/(14 + 5 - 1)$

a procedure. This result for  $A_0^{\pi^+\pi^-}$  being close to what one would obtain through the AQPM rule, we then proceed to perform the fit for  $\pi^-\pi^-$ . The results of the fit to the low energy parameters for  $\pi^-\pi^-$  are given in Table 4. Notice that, both for  $\pi^-\pi^-$  as well as for  $\pi^+\pi^-$ , making the fit in the variable  $s = M_{\pi\pi}^2$  leads to very similar results as those for fits in the variable  $E_{lab}$ . The small error from data reported by [39] compared to those in [36] makes the fit leaning towards the lower numerical results.

As in the case of  $\pi p$  scattering, the high energy part, mini-jets and soft gluon resummation, is then calculated with the same set of parameters as for  $pp$  and  $\bar{p}p$  and  $\pi p$ , namely GRVLO densities,  $p_{tmin} = 1.15$  GeV and  $p = 0.75$ . For  $\pi^-\pi^-$ , at high energy, the effect of the two different fits of the low energy data results in  $\sim 1$  mb difference in the total cross-section at high energy.

Our results for  $\pi^+\pi^-$  and  $\pi^-\pi^-$  are shown in Fig. 4, where we reproduce the data we have found in the literature. In the left panel we compare data for  $\pi^+\pi^-$  with our model predictions as well as with the Regge based parametrizations by Pelaez and Yndurain [28]. We notice the difference in the energy behaviour between our curves and the PY fits. At low energy the difference may be due to our fitting data from  $\sqrt{s} = 2.5$  GeV only. This follows from the fact that we always include in the fits the mini-jet contribution, and the relative PDFs cannot be used at lower energy values. At the same time lack of data in the region where the rise is expected to start reduces the predictive power of fits. This difference, between low energy fits and high energy behaviour from models, makes a measurement of this process particularly interesting.

Finally we compare all the six processes we have examined in this paper. We give the numerical results for some representative energy values in Table 5

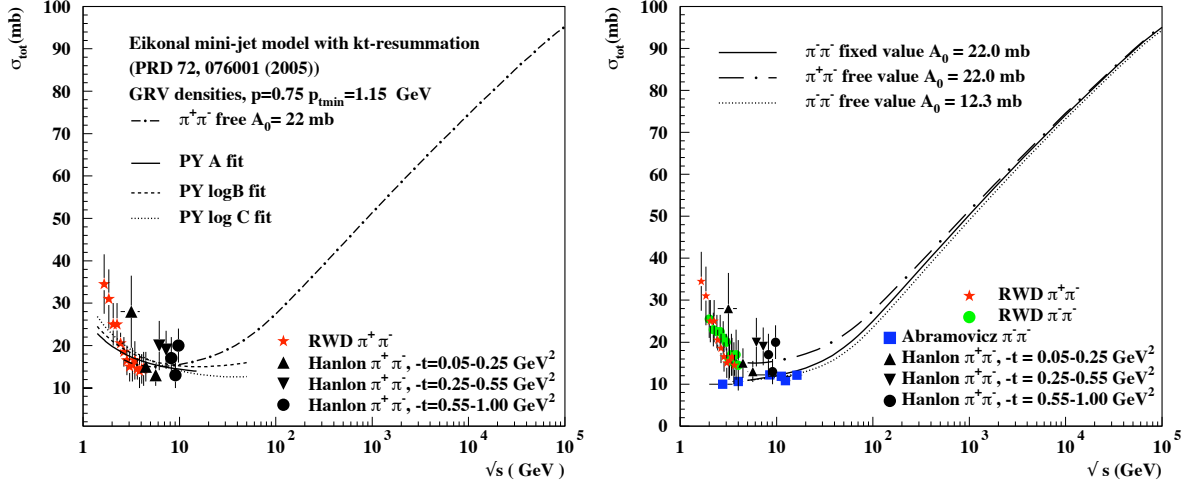


Figure 4: Predictions for  $\pi^+\pi^-$  and  $\pi^-\pi^-$  scattering using our eikonal minijet model are shown. At left our results are compared with the central values of PY [28]. For  $\pi^+\pi^-$  data, the constant term in the fit is given by  $A_0^{\pi\pi} = 22 \text{ mb} \approx 4/9 A_0^{pp}$ . Our predictions for  $\pi^-\pi^-$  using both free and fixed  $A_0$  are also shown. RWD data are from [36], Abramowicz et al. data are from [39], Hanlon et al. data are from [37].

and then show the results in an overall figure. In Table 5, the ratio  $\mathcal{R}$  is calculated from

$$\mathcal{R} = \frac{\langle \sigma_{tot}^{\pi\pi} \rangle_N}{\langle \sigma_{tot}^{\pi\pi} \rangle_{model}} \quad (14)$$

and gives the results of a "factorization" exercise, namely whether our model satisfies factorization for  $\pi\pi$  scattering, with  $\langle \sigma_{tot}^{\pi\pi} \rangle_{model}$  calculated through the values in Table 5 as the average of  $\pi^+\pi^-$  and  $\pi^-\pi^-$ . For the latter, we take the average between free and fixed  $A_0$  parametrizations. Factorization is tested by comparing the model results with the factorized expression obtained

Table 5: Numerical values obtained from our model for proton and pion total cross-sections in mb at selected cm energy values, using central values for the low energy parameters.

$\sqrt{s}$ (GeV)	$pp$	$p\bar{p}$	$\pi^+p$ free $A_0$	$\pi^-p$ free $A_0$	$\pi^+\pi^-$ free $A_0$	$\pi^-\pi^-$ fixed $A_0$	$\pi^-\pi^-$ free $A_0$	$\mathcal{R}$
5	40	51.9	24.3	26	15	10.9	10.8	1.06
100	47.4	47.5	33.8	34	27.5	25	23.1	0.94
1000	70.1	70	58.5	59.0	51.3	50.3	48.9	0.98
10000	97.9	97.8	85.7	86.1	74.6	74.1	73.1	1.02

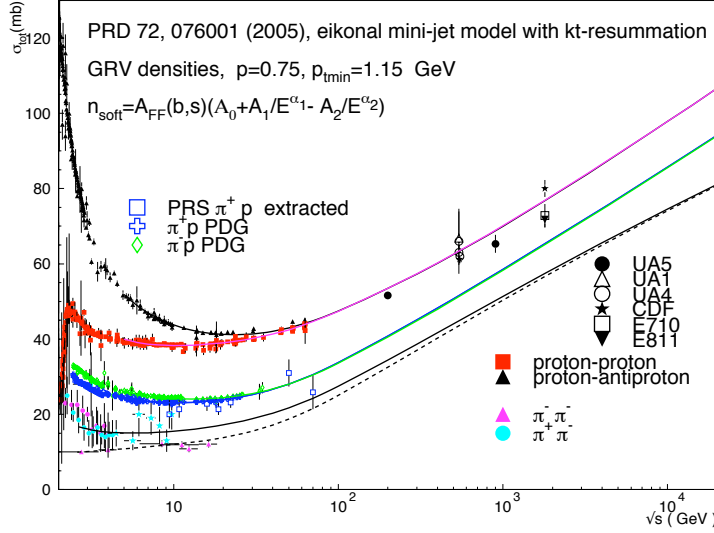


Figure 5: Our curves for  $pp$ ,  $\bar{p}p$ ,  $\pi^\pm p$  and  $\pi\pi$  using the same high energy parameters and densities, and different low energy parametrizations, as described in the text. For  $\pi^-\pi^-$  the (dashed) curve corresponds to fixed  $A_0=22$  mb.

from

$$\langle \sigma_{tot}^{\pi\pi} \rangle_N = \frac{(\sigma_{tot}^{\pi N})^2}{\sigma_{tot}^{NN}} \quad (15)$$

with

$$\sigma_{tot}^{\pi N} = \frac{\sigma^{\pi^+ p} + \sigma^{\pi^- p}}{2}, \quad \sigma_{tot}^{NN} = \frac{\sigma^{pp} + \sigma^{p\bar{p}}}{2} \quad (16)$$

In Fig. 5 we collect the results from our model combining together all proton and pion total cross-sections.

## 5. Conclusion

Our minijet model for total cross-sections for (i)  $NN$  (and  $N\bar{N}$ ), (ii)  $\pi N$  and (iii)  $\pi\pi$  exhibits some general characteristics. In the low-to-medium energy range the quark counting rule works quite well (that is, the ratio  $1 : 2/3 : 4/9$  for the three cases holds). At higher energies, the three cross-sections appear to rise roughly at a similar rate. This analysis confirms the general belief that the quark model is valid at lower energies, whereas, in the asymptotic domain, it gives strong support that our model based on minijets with soft gluon resummation provides an adequate description of all hadronic total cross-sections. Experimentally, the data are most precise for the  $NN$  case and less so for the  $\pi N$  case. Data for pions either do not extend to the region where the rise is well established, as in the case of  $\pi p$ , or are insufficient to make a good fit at low energy, as is the case for  $\pi\pi$ . This does

not allow for reliable fits at very high energy. On the other hand, models can be tested. Our model for the high energy part has the virtue of being of straightforward application, when substituting pions for protons. Once the values for the parameters for  $p$  and  $p_{tmin}$  are chosen, the PDFs available for the particles under consideration provide the mini-jet cross-section and the soft scale  $q_{max}$  for the  $b$ -distribution. Clearly, measurements at LHC for pion reactions would be most useful.

## Acknowledgments

O.S. is grateful to S. Eydelman of Novosibirsk for enlightening conversations about pion data, and G.P. thanks M. Murray, CMS, U. of Kansas, for discussions about the planned ZDC measurements and R. Pelaez and Jacobo Ruiz de Elvira from U. Madrid for helping us with data from the Pelaez and Yndurain fits.. G.P. gratefully acknowledges the hospitality of the Center for Theoretical Physics of MIT and Brown U. Physics Department. Y.S. would like to thank the Physics Department for his stay as an Emeritus Professor at Northeastern University, Boston. Work partially supported by the Spanish MEC (FPA2006-05294 and FPA2008-04158-E/INFN) and by Junta de Andalucía (FQM 101).

## References

- [1] A. Corsetti, A. Grau, G. Pancheri, Y. N. Srivastava, Bloch-Nordsieck summation and partonic distributions in impact parameter space, Phys. Lett. B382 (1996) 282–288.
- [2] A. Grau, R. M. Godbole, G. Pancheri, Y. N. Srivastava, Soft gluon kt-Resummation and the Froissart bound, Phys. Lett. B682 (2009) 55–60.
- [3] V. A. Petrov, R. A. Ryutin, A. E. Sobol, LHC as  $\pi p$  and  $\pi\pi$  Collider, Eur. Phys. J. C65 (2010) 637–647.
- [4] P. Lebiedowicz, A. Szczurek, Exclusive  $pp \rightarrow nn\pi^+\pi^+$  reaction at LHC, arxiv:hep-ph/1005.2309 (2010).
- [5] A. E. Sobol, R. A. Ryutin, V. A. Petrov, M. Murray, Elastic  $\pi^+p$  and  $\pi^+\pi^+$  scattering at LHC, arxiv: hep-ph/1005.2984 (2010).

- [6] O. A. Grachov, et al., Performance of the combined zero degree calorimeter for CMS, J. Phys. Conf. Ser. 160 (2009) 012059.
- [7] P. Soding, On the Apparent shift of the rho meson mass in photoproduction, Phys. Lett. 19 (1966) 702–704.
- [8] M. G. Ryskin, Y. M. Shabelski, Role of a nonresonance background in the diffractive electro- and photoproduction of rho0 mesons, Phys. Atom. Nucl. 61 (1998) 81–86.
- [9] J. Breitweg, et al., Elastic and proton dissociative  $\rho^0$  photoproduction at HERA, Eur. Phys. J. C2 (1998) 247–267.
- [10] W. Flauger, F. Monnig, Measurement of Inclusive Zero-Angle Neutron Spectra at the ISR, Nucl. Phys. B109 (1976) 347.
- [11] V. A. Khoze, A. D. Martin, M. G. Ryskin, Information from leading neutrons at HERA, Eur. Phys. J. C48 (2006) 797–804.
- [12] A. B. Kaidalov, V. A. Khoze, A. D. Martin, M. G. Ryskin, Leading neutron spectra, Eur. Phys. J. C47 (2006) 385–393.
- [13] B. Z. Kopeliovich, I. K. Potashnikova, I. Schmidt, J. Soffer, Damping of forward neutrons in  $pp$  collisions, Phys. Rev. D78 (2008) 014031.
- [14] S. Chekanov, et al., Leading neutron production in  $e^+ p$  collisions at HERA, Nucl. Phys. B637 (2002) 3–56.
- [15] S. Chekanov, et al., Leading neutron energy and  $p(T)$  distributions in deep inelastic scattering and photoproduction at HERA, Nucl. Phys. B776 (2007) 1–37.
- [16] D. Varga, Baryon number transfer and baryon pair production in soft hadronic interactions at the CERN SPS, Eur. Phys. J. C33 (2004) s515–s517.
- [17] G. Anelli, et al., The TOTEM experiment at the CERN Large Hadron Collider, JINST 3 (2008) S08007.
- [18] F. Bloch, A. Nordsieck, Note on the Radiation Field of the electron, Phys. Rev. 52 (1937) 54–59.



- [19] D. Cline, F. Halzen, J. Luthe, High transverse momentum secondaries and rising total cross-sections in cosmic ray interactions, *Phys. Rev. Lett.* 31 (1973) 491–494.
- [20] G. Pancheri, Y. Srivastava, M. Pallotta, KNO scaling violations and the appearance of the three gluon coupling at the collider, *Phys. Lett.* B151 (1985) 453.
- [21] L. Durand, P. Hong, QCD and Rising Total Cross-Sections, *Phys. Rev. Lett.* 58 (1987) 303–306.
- [22] L. Durand, H. Pi, Semihard QCD and high-energy p p AND anti-p p scattering, *Phys. Rev.* D40 (1989) 1436.
- [23] T. Sjostrand, M. van Zijl, A Multiple Interaction Model for the Event Structure in Hadron Collisions, *Phys. Rev.* D36 (1987) 2019.
- [24] P. Lipari, M. Lusignoli, Multiple Parton Interactions in Hadron Collisions and Diffraction, *Phys. Rev.* D80 (2009) 074014.
- [25] A. Grau, G. Pancheri, Y. N. Srivastava, Hadronic total cross-sections through soft gluon summation in impact parameter space, *Phys. Rev.* D60 (1999) 114020.
- [26] R. M. Godbole, A. Grau, G. Pancheri, Y. N. Srivastava, Soft gluon radiation and energy dependence of total hadronic cross-sections, *Phys. Rev.* D72 (2005) 076001.
- [27] M. Gluck, E. Reya, A. Vogt, Parton distributions for high-energy collisions, *Z. Phys.* C53 (1992) 127–134.
- [28] J. R. Pelaez, F. J. Yndurain, Regge analysis of pion pion (and pion kaon) scattering for energy  $\sqrt{s} > 1.4 \text{ GeV}$ , *Phys. Rev.* D69 (2004) 114001.
- [29] F. J. Yndurain, The quadratic scalar radius of the pion and the mixed  $\pi - K$  radius, *Phys. Lett.* B578 (2004) 99–108.
- [30] C. Amsler, et al., Review of particle physics, *Phys. Lett.* B667 (2008) 1.
- [31] A. Donnachie, P. V. Landshoff, Total cross-sections, *Phys. Lett.* B296 (1992) 227–232.

- [32] M. M. Block, F. Halzen, New evidence for the saturation of the Froissart bound, *Phys. Rev. D* 72 (2005) 036006.
- [33] M. Gluck, E. Reya, A. Vogt, Pionic parton distributions, *Z. Phys. C* 53 (1992) 651–656.
- [34] N. N. Biswas, N. M. Cason, I. Derado, V. P. Kenney, J. A. Poirier, W. D. Shephard, Total pion-pion cross sections for the 2-gev di-pion mass region, *Phys. Rev. Lett.* 18 (1967) 273–276.
- [35] D. Cohen, T. Ferbel, P. Slattery, B. Werner, Study of  $\pi\pi$  scattering in the isotopic-spin-2 channel, *Phys. Rev. D* 7 (1973) 661–668.
- [36] W. J. Robertson, W. D. Walker, J. L. Davis, High-energy  $\pi\pi$  collisions, *Phys. Rev. D* 7 (1973) 2554–2564.
- [37] J. Hanlon, et al., The Inclusive Reactions  $p n \rightarrow p X$  and  $\pi^+ n \rightarrow p X$  at 100-GeV/c, *Phys. Rev. Lett.* 37 (1976) 967.
- [38] W. Hoogland, et al., Measurement and Analysis of the  $\pi^+ \pi^+$  System Produced at Small Momentum Transfer in the Reaction  $\pi^+ p \rightarrow \pi^+ \pi^+ n$  at 12.5-GeV, *Nucl. Phys. B* 126 (1977) 109.
- [39] H. Abramowicz, et al., Study of  $\pi^- \pi^-$  scattering in  $\pi^- n$  interactions at high-energies, *Nucl. Phys. B* 166 (1980) 62.